www.czasopisma.pan.pl PAN www.journals.pan.pl

VERSITA

Arch. Min. Sci., Vol. 58 (2013), No 2, p. 495–504

Electronic version (in color) of this paper is available: http://mining.archives.pl

DOI 10.2478/amsc-2013-0033

SEYED SALEH BEHBAHANI*[1], PARVIZ MOAREFVAND**, KAVEH AHANGARI*, KAMRAN GOSHTASBI***

MEASURING DISPLACEMENT AND CONTACT FORCES AMONG THE PARTICLES IN UNLOADING OF SLOPE BY PFC2D (PARTICLE FLOW CODE)

POMIARY PRZEMIESZCZEŃ I SIŁ KONTAKTU POMIĘDZY CZĄSTKAMI MATERIALNYMI W TRAKCIE WYBIERANIA WYROBISKA POCHYŁEGO PRZY POMOCY PROGRAMU PFC2D

When instability is observed in the walls of open pit mining, at this time, engineers are faced with a moving mass which is a combination of materials that move on each other and on the main slip surface. Modeling of this movement can have an effective assistance to mining engineers to predict the movement behavior, displacement estimate, and the moving volumes. One of the suitable software which is capable of modeling of sliding behavior is PFC (Particle Flow Code). It is based on Discrete Element Method and released by the Itasca Company. In this paper, the modeling of sliding mass and unloading it in seven stages have been done. During the seven stages of unloading the maximum displacement and maximum contact forces among the particles are obtained. Maximum displacement happened in the fifth stage of the unloading and it is equal to 134.8 meters. Maximum contact forces occurred in the first stage of the unloading after initial equilibrium stage and it is equal to 1917 kN. The model for unloading of sliding mass presented in this paper is just an example and it is not a definite model for unloading of each sliding mass. Unloading of sliding mass depends on the situation of sliding mass and its volume and also mining limitations.

Keyword: Unloading, Discrete Element Method (DEM), Sliding Mass, PFC2D

W przypadku wystąpienia niestabilności ścian pochyłego wyrobiska odkrywkowego, inżynierowie mają do czynienia z przemieszczającą się masa – będącą kombinacją materiałów przesuwających się względem siebie a także zsuwających się w dół po powierzchni spadu. Modelowanie tego ruchu może znacznie pomóc inżynierom-górnikom w prognozowaniu zachowań terenu w trakcie tego ruchu, do szacowania wielkości przemieszczeń i objętości przemieszczających się mas materiału. Jednym z programów wspomagających modelowanie przemieszczeń tego typu jest oprogramowanie Particle Flow Code PFC, rozprowadzane przez firmę Itasca, wykorzystujące metodę elementów dyskretnych. W pracy tej

* DEPARTMENT OF MINING ENGINEERING, SCIENCE AND RESEARCH BRANCH, ISLAMIC AZAD UNIVERSITY, TEHRAN, IRAN.
** DEPARTMENT OF MINING AND METALLURGY, AMIRKABIR UNIVERSITY OF TECHNOLOGY, IRAN.
** DEPARTMENT OF MINING ENGINEERING, TARBIAT MODARES UNIVERSITY, TEHRAN, IRAN.
[1] CORRESPONDING AUTHOR: E-mail: salehbehbahani@yahoo.com

przeprowadzono modelowanie ruchu przesuwających się mas gruntu i wybierania wyrobiska pochyłego w siedmiu etapach. We wszystkich siedmiu etapach modelowania obliczono maksymalne przemieszczenia i siły kontaktowe pomiędzy cząstkami gruntu. Maksymalne przemieszczenia zarejestrowano w etapie piątym wybierania wyrobiska pochyłego, wyniosło ono 134.8 m. Maksymalna siła kontaktowe, która wystąpiła w etapie pierwszym po ustaniu pierwotnego stanu równowagi, wyniosła 1917 kN. Model wybierania przesuwającej się masy gruntu przedstawiony w pracy jest jedynie przykładem, nie jest to ścisły model mający zastosowanie do modelowania ruchu przesuwających się mas gruntu w trakcie wybierania. Wybieranie przesuwających się mas gruntu zależy od warunków przemieszczania się masy gruntu, jej objętości a także ograniczeń narzuconych przez uwarunkowania górnicze.

Słowa kluczowe: wybieranie, metoda elementów dyskretnych, przemieszczające się masy gruntu

1. Discrete Element Method

Classical Discrete Element Method (DEM) was proposed by Cundall and Strack (1979). The Discrete Element Method has been applied to many cases for solving problems involving many discontinuous materials such as soil and rock. This method is especially appropriated for the simulation of granular and particle systems. Continuum methods need very complex models, involving many parameters for simulation of sophisticated behaviors for soil and rock. Compared with continuum methods, a DEM model requires only a few material properties because the behavioral complexity such as nonlinear stress/strain response, dilation phenomena, transition from brittle to ductile behavior, nonlinear strength envelopes arises automatically (Cundall, 2002).

2. Particle Flow Code (PFC2D)

PFC2D is one of the most efficient tools to model complicated problems in solid mechanics and granular flow. Some researches have been done by PFC software, and also some papers have been submitted to different journals by Chang et al. (2011), He et al. (2010), Jackson et al. (2008), Liu and Koyi (2012), Poisel et al. (2009), Thompson et al. (2009), Wang et al. (2003), Ghazvinian et al. (2012), Asadi et al. (2012). This software is used to model the movements and interactions of spherical particles using the Distinct Element Method. In this method, objects are shown as discrete rigid particles (balls) which can be bonded by parallel bonds or contact bonds. The bond has shear and normal strength components. The contact stiffness between any two particles can be measured by normal and shear stiffness. Parallel bonds can move both forces and moments among the particles, while contact bonds can move just forces that are acting at the contact point. A slip-model, determined by a friction coefficient between any two particles, forms the frictional strength characteristic of the assemblies. Fracturing can be carried out by bond breaking in either shear mode or normal mode. Jointed rock block behavior can be simulated by assemblies of clumps or clusters.

3. Divided Zones

This model is considered in four different zones which described below:

- Sheared zone is modeled with about 1335 balls,
- Sliding zone is modeled with about 6325 balls,

- Crushed zone is modeled with about 3713 balls,
- Debris zone is located in the lowest part of pit. This zone is modeled with about 2268 balls.

The initial sliding mass model is given in Figure 1.

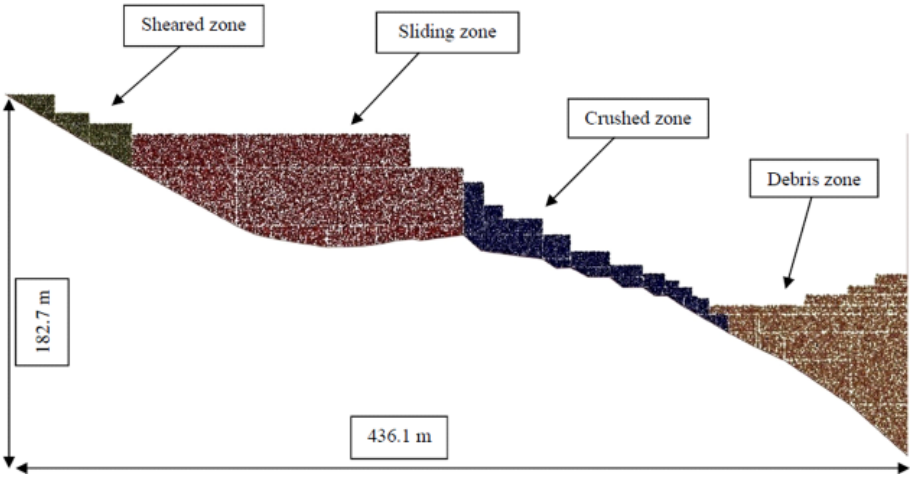

Fig. 1. The initial sliding mass model

4. Modeling of sliding mass and unloading it by PFC2D

Sliding mass has been modeled by PFC2D and then unloading of sliding mass in the seven stages have been done.

Slip surface is shown in the modeling as walls and sliding mass is located on the walls. Walls properties are similar to mass in-situ. A clump is located between the walls and the sliding mass. Sliding mass can slide on the clump. Balls and walls properties are given in Tables 1 and 2, respectively.

TABLE 1

Balls properties used in the modeling

Zones	Density (Kg/m^3)	s-bond (N)	n-bond (N)	Friction angle (degree)	K_s (N/m)	K_n (N/m)	Max. radius (mm)	Min. radius (mm)
clump	1800	1e8	3e5	14	1e5	1e8	75	75
Sheared	2500	5e7	15e4	21	5e4	5e7	300	250
Sliding	2000	2e8	6e5	23	2e5	2e8	500	250
Crushed	2500	5e7	15e4	14	5e4	5e7	300	250
Debris	2500	5e7	15e4	14	5e4	5e7	550	500

s-bond: Contact bond shear strength; n-bond: Contact bond normal strength

TABLE 2

Walls properties used in the modeling

K_n (N/m)	K_s (N/m)	Friction angle (degree)
1e10	1e7	11

K_n: Normal stiffness; K_s: Shear stiffness

Unloading in the first to fourth stages of the debris zone, and also in the fifth and sixth stages of crushed zone has been done. Unloading has occurred in the seventh stage of the crushed and sliding zones. In Figure 2, the stage which initial sliding has reached the equilibrium, and also the unloading of sliding mass in the seven stages, are shown. In the fourth stage, the debris zone has been completely removed.

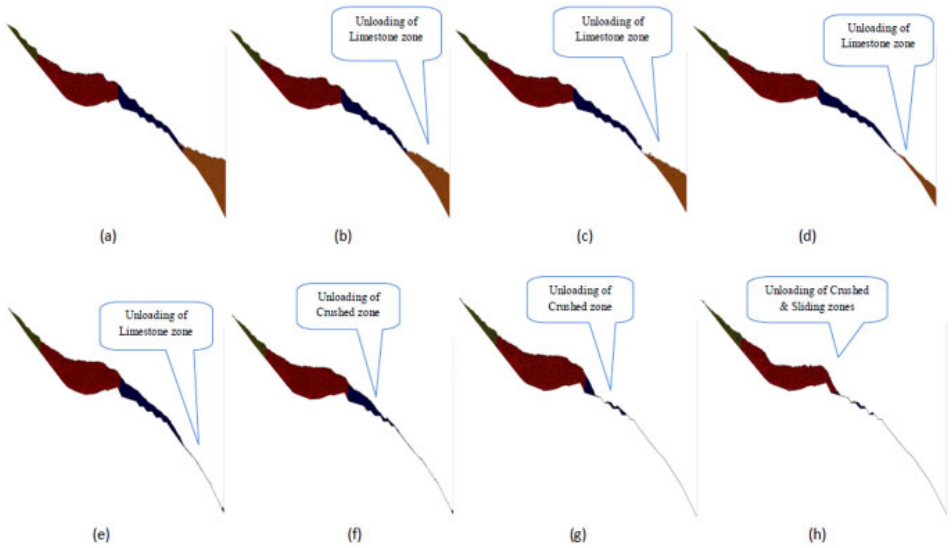

Fig. 2. (a) The stage that initial sliding has reached the equilibrium and unloading in the (b) first, (c) second, (d) third, (e) fourth, (f) fifth (g) sixth and (h) seventh stages, are shown

In the seventh stage of unloading, the model has not reached the equilibrium yet and the displacements are still continued. In Figure 3, due to better monitoring surface and subsurface of sliding mass, the sheared zone divided in two parts A and A1, the sliding zone divided in two parts B and B1, the crushed zone divided in two parts C and C1, and the debris zone divided in two parts D and D1. During the modeling, displacements of each part are obtained.

Figures 4 and 5 show displacement vectors with particles in the initial equilibrium stage and in the third stage of the unloading, respectively. As shown in these figures, the vectors of each ball that are larger, the ball displacement is also higher.

Figures 6 and 7 show contact forces among the particles in the initial equilibrium stage and in the seventh stage of the unloading, respectively.

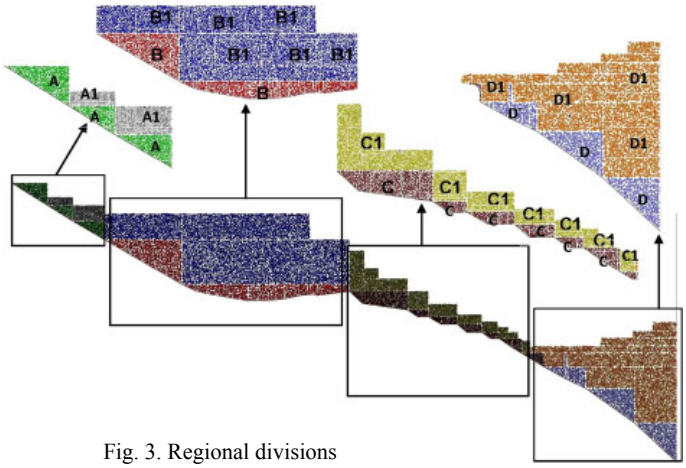

Fig. 3. Regional divisions

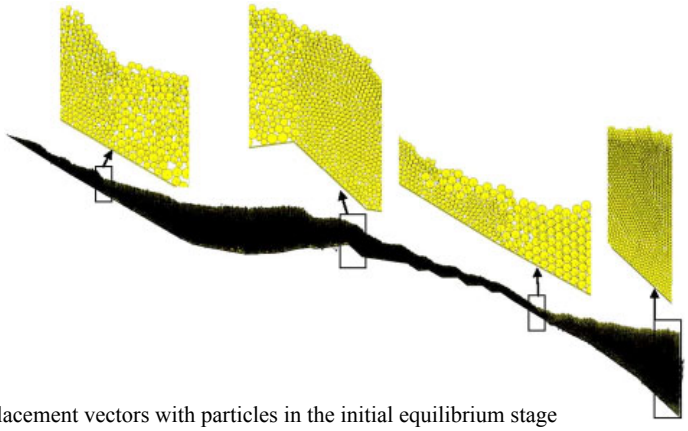

Fig. 4. Displacement vectors with particles in the initial equilibrium stage

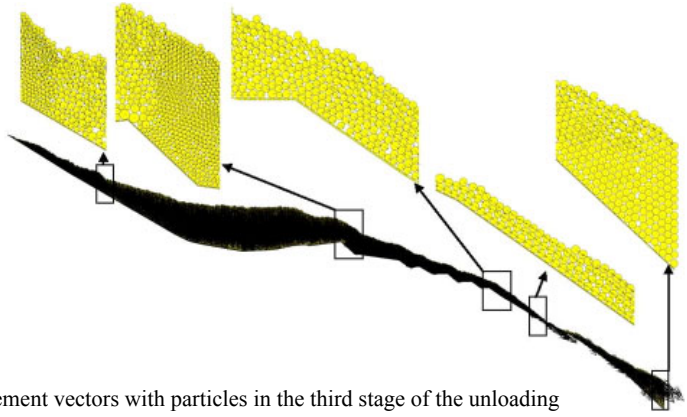

Fig. 5. Displacement vectors with particles in the third stage of the unloading

These Figures indicates in each part, which has thicker black lines, the contact forces between the balls are more than the other parts.

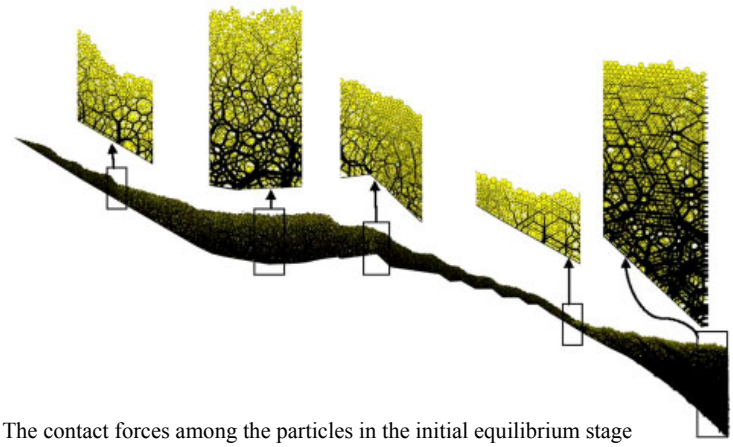

Fig. 6. The contact forces among the particles in the initial equilibrium stage

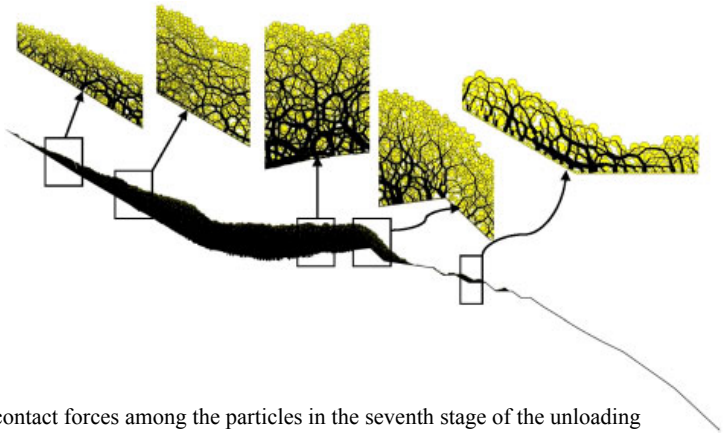

Fig. 7. The contact forces among the particles in the seventh stage of the unloading

5. Results

In Figure 8, the maximum values of displacement in the initial equilibrium stage and in the seven stages of the unloading are shown; and also in Table 3 the maximum numerical values are shown.

In the fifth stage of unloading due to the removal of the crushed zone and decreasing the weight on the toe at the bottom of slope, the maximum displacement occurred in this stage. In Figure 9, the maximum values of displacement in the initial equilibrium stage and in the seven stages of the unloading are shown; and also in Table 4 the maximum numerical values are shown.

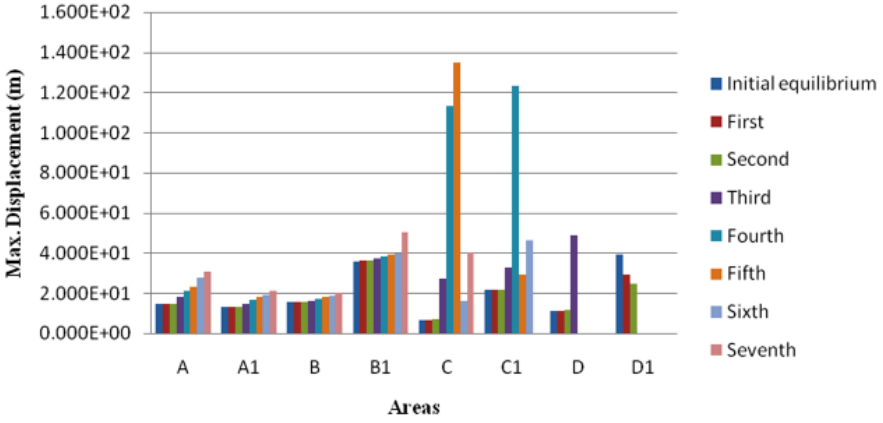

Fig. 8. The maximum values of displacement (m) in each area of the initial equilibrium stage and in the seven stages of the unloading

TABLE 3

The maximum numerical values of displacement (m) in each area of the initial equilibrium stage and in the seven stages of the unloading

Areas / Unloading stages	A	A1	B	B1	C	C1	D	D1
Initial equilibrium	14.73	13.3	15.6	35.97	6.632	21.41	11.17	39.46
First	14.75	13.31	15.63	35.99	6.658	21.45	11.19	29.38
Second	14.76	13.33	15.63	36	6.812	21.48	11.51	24.85
Third	17.93	14.83	16.34	37.27	27.01	32.47	48.96	NA
Fourth	20.98	16.52	17.22	38.21	113	123.4	NA	NA
Fifth	23.35	18.05	18.06	39.07	134.8	29.37	NA	NA
Sixth	27.86	19.11	18.6	39.68	15.9	46.35	NA	NA
Seventh	30.79	21.24	0.0000611	0.001069	40.35	NA	NA	NA

TABLE 4

The maximum numerical values of displacement in the initial equilibrium stage and in the seven stages of the unloading

Stages of unloading	Max. Displacement (m)	Regions
Initial equilibrium	39.46	D1
First	35.99	B1
Second	36	B1
Third	48.96	D
Fourth	123.4	C1
Fifth	134.8	C
Sixth	46.35	C1
Seventh	50.27	B1

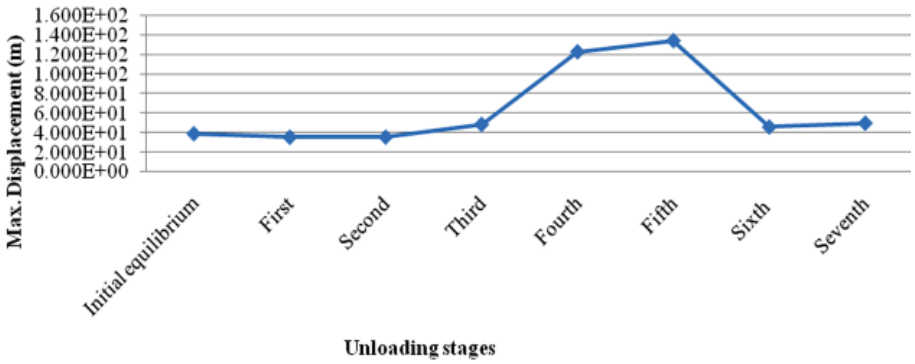

Fig. 9. The maximum values of displacements in the initial equilibrium stage and in the seven stages of the unloading

In the fourth and seventh stages of the unloading, the contact forces are 627.5 and 634.2 (kN), respectively. The contact forces decreased up to the fourth stage, but the contact forces increased in the fifth stage of unloading again. This is due to the unloading of the crushed zone.

In Table 5 and the Figures 10, maximum values of contact forces in the initial equilibrium stage and in the seven stages of unloading are shown.

TABLE 5

The maximum values of contact forces in the initial equilibrium stage and in the seven stages of the unloading

Values / Unloading stages	Max. Contact forces (N)
Initial equilibrium	2236000
First	1917000
Second	1760000
Third	1347000
Fourth	627500
Fifth	859800
Sixth	795100
Seventh	634200

6. Conclusion

- The model which has been presented in this paper is just an example for unloading of sliding mass. It is not a definite model for unloading of each sliding mass. It is obvious that unloading of sliding mass depends on the different situations, for instance, its volume of sliding mass and mining limitations.

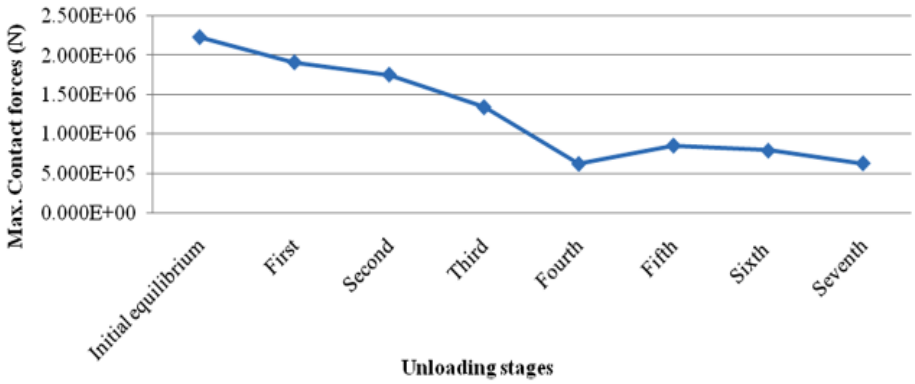

Fig. 10. The maximum values of contact forces in the initial equilibrium stage and in the seven stages of the unloading

- Maximum displacement is in C region and in the fifth stage of the unloading and it is equal to 134.8 meters. Also, maximum contact forces after initial equilibrium stage are related to first stage of the unloading and equal to 1917 (kN).
- Sliding mass in the modeling after the seventh stage of unloading does not reach the equilibrium and is moving.
- The way which we can deal with the sliding mass is to remove it completely. Obviously, before the sliding mass, the benches which are near to the bedrock and now are under the rubble are destroyed. It is because of rubble falling on them and need to rebuild in the bedrock.

References

Asadi M.S., Rasouli V., Barla B., 2012. *A Bonded Particle Model Simulation of Shear Strength and Asperity Degradation for Rough Rock Fractures*. Rock Mech. Rock Eng.

Ghazvinian A., Sarfarazi V., Schubert W., Blumel M., 2012. *A Study of the Failure Mechanism of Planar Non-Persistent Open Joints Using PFC2D*. Rock Mech. Rock Eng.

Cundall P.A., Strack O.D.L., 1979. *A Discrete Numerical Model for Granular Assemblies*. Geotechnique, Vol. 29. pp. 47-65.

Cundall P.A., 2002. *A Discontinuous Future for Numerical Modeling in Soil and Rock. Discrete Element Methods – Numerical Modeling of Discontinua*. Ed. Cook B. K. and Jensen R. P. Geotechnical Special Publication, No. 117.

Chang K.T., Lin M.L., Dong J.J., Chien C.H., 2011. *The Hungtsaiping Landslides: From Ancient to Recent*. Landslides.

He J., Li X., Li S., Yin Y., Qian H., 2010. *Study of Seismic Response of Colluvium Accumulation Slope by Particle Flow Code*. Granular Matter.

Jackson K., Kingman S.W., Whittles D.N., Lowndes I.S., Reddish D.J., 2008. *The Effect of Strain Rate on the Breakage Behaviour of Rock*. Arch. Min. Sci., Vol. 53, No 1, p. 3-22.

Liu Z., Koyi H., 2012. *Kinematics and Internal Deformation of Granular Slopes: Insights from Discrete Element Modeling*. Landslides.

Poisel R., Angerer H., Pöllinger M., Kalcher T., Kittl H., 2009. *Mechanics and Velocity of the Lärchberg – Galgenwald Landslide (Austria)*. Engineering Geology.

Thompson N., Bennett M., Petford N., 2009. *Analyses on Granular Mass Movement Mechanics and Deformation with Distinct Element Numerical Modeling: Implications for Large-Scale Rock and Debris Avalanches*. Acta Geotechnica.

Wang C., Tannant D.D., Lilly P.A., 2003. *Numerical Analysis of the Stability of Heavily Jointed Rock Slopes Using PFC2D*. International Journal of Rock Mechanics & Mining Sciences.

Received: 28 May 2012